

# A New Digital Signal Processing Implementation of OFDM Timing Recovery

Yi-Ching Liao, Kwang-Cheng Chen

Institute of Communications Engineering, College of Electrical Engineering  
National Taiwan University, Taipei, Taiwan, 10617, R.O.C.

FAX: +886-2-23683834

E-mail: ycliao@santos.ee.ntu.edu.tw, chenkc@cc.ee.ntu.edu.tw

*Abstract*—In this paper, we present a novel and pure digital timing recovery scheme in orthogonal frequency division multiplexing (OFDM) system without additional pilots. This optimum estimator is derived based on the maximum likelihood (ML) criterion with the decision directed approach. Sub-optimum schemes based on correlation extraction and SCCL algorithm are also developed. Simulations show that the estimation variance of the optimum scheme approaches zero for signal-to-noise ratio greater than 6 dB with number of subcarriers equals to 256. And the SCCL-based sub-optimum scheme is simpler and efficient to apply in closed loop operation.

## I. INTRODUCTION

In recent years, with the growing demand for wireless Internet access and wireless multimedia services, considerable attention has been focused on the design of broadband wireless communication system to support high rate transmission up to tens or hundreds of Mbps with high carrier frequency at the level of GHz. In such condition, the channel is generally frequency selective and dispersive which causes serious performance degradation and impairment (inter-symbol interference, for instance) to reliable transmission of a broadband signal. Adaptive equalization techniques can be used to correct this distortion. However, for data rates up to tens of Mbps, adaptive equalization introduces practical difficulties for compact size and low power consumption.

OFDM which was proposed by Chang [10] is a principle for transmitting information via a synthesis of multiple band-limited signals through a linear band-limited channel without inter-symbol interference (ISI) and inter-channel interference (ICI). Enhancements such as using digital Fourier transform (DFT) to perform baseband modulation [11] and demodulation and introducing cyclic prefix to maintain the orthogonality [12] make OFDM more attractive.

The main advantage of OFDM is its capability of multi-fold increasing the symbol duration. With the increase of the number of subcarriers, the frequency selectivity of the channel may be reduced so that each subcarrier experiences flat fading. Consequently, the complexity of channel

This paper was supported by the Ministry of Education under the project contract 89-E-FA06-2-4.

equalization can be greatly reduced. OFDM has been suggested for a variety of applications such as asymmetric digital subscriber loop (ADSL) and very high bit rate digital subscriber loop (HDSL) [9] in telephone network, digital audio broadcasting (DAB) [8] and digital video broadcasting (DVB) [2] in broadcasting system and mobile communication systems [7]. And the most important application for future wireless multimedia is high speed data transmission over fading channels.

In OFDM, orthogonality is obtained by having the sub-carrier spacing as the baud rate, and having the FFT demodulation process accumulate over exactly one OFDM symbol. However, the orthogonality can only occur if the demodulator clock is synchronized to modulator and no frequency offset is present. If a timing offset occurs, it will cause a phase rotation which has been analyzed in [12]. Therefore, it is extremely important to estimate the exact timing offset to force the receiver to start its FFT processor at the right time and mitigate the effect of phase rotation.

Another critical problem of OFDM transceiver is that the synchronization scheme introduces significant complexity and is difficult to implement. It is extremely important to find out a synchronization scheme which is simple, effective and compatible with DSP realization of OFDM. Hence, we start from the ML-sense optimum approach for timing synchronization in ideal OFDM system, and then derive sub-optimum architectures from the optimum scheme based on correlation extraction and SCCL algorithm [6] which is simple and proved an effective tracking scheme for symbol timing. In Section II, the OFDM transmission model is described. The synchronization methods both the optimum approach and the sub-optimum approaches are presented in Section III. Performance simulation and conclusion are contained in Section IV and V respectively.

## II. OFDM SYSTEM MODEL

The OFDM transmitted baseband complex signal can be written as

$$s(t) = \frac{1}{N} \sum_{l=-\infty}^{+\infty} \sum_{k=0}^{N-1} X_{l,k} e^{j2\pi f_k t} g(t - lT) \quad (1)$$

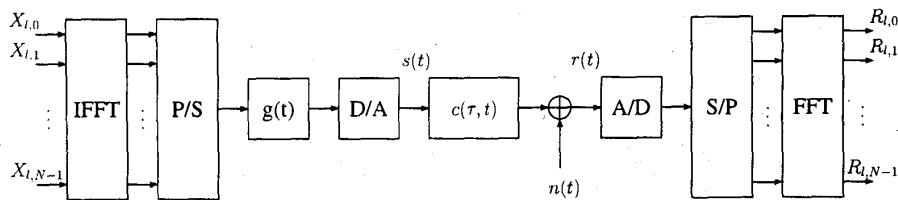


Fig. 1. Block diagram of OFDM transmission system.

where  $f_k = \frac{k}{T}$ ,  $T$  is the OFDM symbol duration,  $X_{l,k}$  is the complex symbol modulating the  $k^{\text{th}}$  carrier with frequency  $f_k$ , at the  $l^{\text{th}}$  time slot of duration  $T$ ,  $N$  is the number of subcarriers and  $g(t)$  the rectangular pulse given by

$$g(t) = \begin{cases} 1 & \text{if } t \in [0, T] \\ 0 & \text{otherwise} \end{cases} \quad (2)$$

The block diagram of an OFDM transmission system is illustrated in Fig. 1.

The transmitted data symbols are modulated on  $N$  subcarriers via an *inverse* FFT processor. After parallel to serial conversion, digital to analog conversion and transmission pulse filtering, the complex baseband transmitted signal  $s(t)$  is obtained. The channel response  $c(\tau, t)$  is assumed to affect  $s(t)$  by a delay  $\tau \in [0, T]$  and a complex, AWGN,  $n(t)$ , i.e.,  $c(\tau, t) = \delta(t - \tau)$ . At the receiving end, the inverse signal processing is performed on the received signal  $r(t)$ . As shown in Fig. 1, after analog to digital conversion and serial to parallel conversion,  $N$  baseband time domain samples are applied to a FFT processor to get the received data symbols  $\{R_{l,0}, \dots, R_{l,N-1}\}$ .

### III. SYNCHRONIZATION METHODS

#### A. Optimum Approach Based on ML Criterion

When *a priori* information about the estimated parameter is not available, the maximum likelihood estimation (MLE) [4] is often applied. Different from conventional ML timing estimator for OFDM, we develop a new version of the optimum symbol timing offset estimator based on ML criterion with decision directed approach. The proposed optimum timing estimation based on MLE is to test all possible candidates simultaneously in present OFDM symbol and choose the parameter with the largest likelihood function value as the estimation for next symbol timing.

Under our assumption, the received complex signal is

$$r(t) = \frac{1}{N} \sum_{n=-\infty}^{+\infty} \sum_{k=0}^{N-1} X_{n,k} e^{j2\pi f_k(t-\tau)} g(t - \tau - nT) + n(t) \quad (3)$$

where  $n(t)$  is the complex additive white Gaussian noise. Based on ML criterion [5], we can derive the log-likelihood

function corresponds to the  $l^{\text{th}}$  symbol.

$$\Lambda_L^l(\tau) = \frac{2}{N} \sum_{k=0}^{N-1} \Re[R_{l,k}^*(\tau) Y_{l,k}(\tau)] - \int_{IT}^{(l+1)T} |r(t + \tau)|^2 dt \quad (4)$$

where  $Y_{l,k}$  is given by

$$Y_{l,k}(\tau) = \int_{IT}^{(l+1)T} r(t + \tau) e^{-j2\pi f_k t} dt \quad (5)$$

The detailed derivation is shown in appendix. And the decision directed optimum symbol timing estimator and the  $n^{\text{th}}$  branch of it are shown in Fig. 2 and Fig. 3 respectively. The optimum symbol timing estimator can be implemented by dividing the observation interval  $(0, T]$  into  $N$  sub-intervals and each interval corresponds to a timing candidate  $\tau_n$ ,  $n \in \{0, 1, \dots, N-1\}$ . After all the log-likelihood functions corresponding to each candidate are calculated, we choose the one with the largest log-likelihood function as the estimated timing.

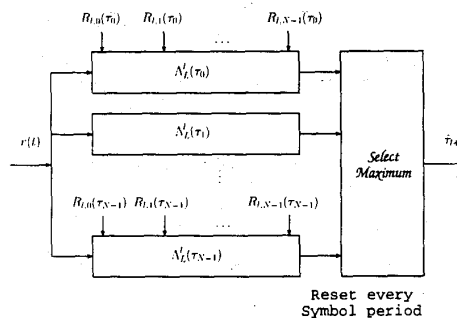


Fig. 2. Block diagram of the optimum synchronizer.

We can convert proposed optimum synchronization scheme to an equivalent digital counterpart. It proceeds by the following approximation.

$$Y_{l,k}(\tau) = \sum_{n=0}^{N-1} r[lN + n + \tau] e^{-j2\pi \frac{kn}{N}} \quad (6)$$

$$\int_{IT}^{(l+1)T} |r(t + \tau)|^2 dt = \sum_{n=0}^{N-1} |r[lN + n + \tau]|^2 \quad (7)$$

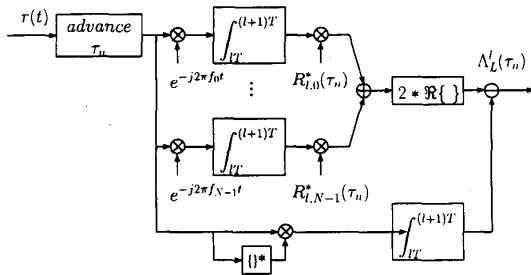


Fig. 3. Block diagram of the  $n^{\text{th}}$  branch in the optimum synchronizer.

Where  $r[lN + n]$  denotes the  $n^{\text{th}}$  digital sample in the  $l^{\text{th}}$  symbol period from the analog to digital converter at the receiver.

From this approximation,  $Y_{l,k}(\tau)$  is exactly the  $k^{\text{th}}$  spectral element of the discrete Fourier transform of  $\{r[lN + \tau], \dots, r[(l+1)N + \tau - 1]\}$ . Thus, we can use FFT to calculate  $Y_{l,k}(\tau)$  and a moving sum unit to calculate the power in (7). The pure DSP realization of the proposed optimum synchronization is illustrated in Fig. 4. The proposed structure can be operated as an open loop system.

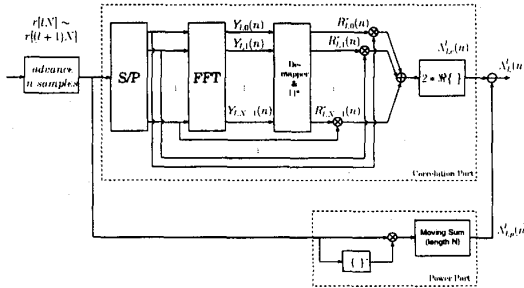


Fig. 4. Block diagram of the digital realization of the  $n^{\text{th}}$  branch in the optimum synchronizer.

### B. Sub-optimum Approach Based on Correlation Extraction

As shown in Fig. 4, the log-likelihood function in each branch of the optimum synchronizer is exactly composed of two individual parts: one is the correlation calculating part, the other is the power calculating part. The relationship of the two constituting part is

$$\Lambda_L^l(n) = \Lambda_{L_c}^l(n) - \Lambda_{L_p}^l(n) \quad (8)$$

where  $\Lambda_{L_c}^l(n)$  denotes the output of the correlation calculating part and  $\Lambda_{L_p}^l(n)$  is the output of the power calculating part. Consequently, it motivates us to investigate the waveforms of the three log-likelihood functions in equation (8) to see if we can extract any information for a simplified implementation of the optimum synchronizer. A simula-

tion result of the waveforms mentioned above with the assumption of 64 subcarriers and QPSK modulation without noise is shown in Fig. 5.

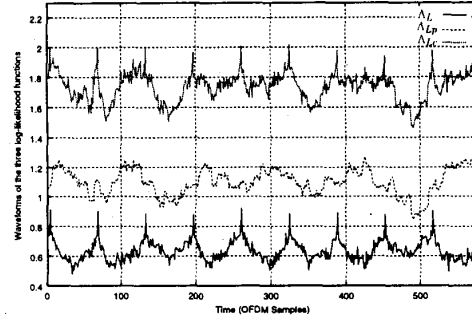


Fig. 5. The waveforms of the three log-likelihood functions with  $N=64$ , QPSK modulation without noise, timing offset = 1/16 symbol period.

After comparing the waveforms of the three log-likelihood functions, we can find that  $\Lambda_{L_c}^l(n)$ , like  $\Lambda_L^l(n)$ , generates periodic peak with period equals to the OFDM symbol duration, although it contains the perturbation of signal power which equals to  $\Lambda_{L_p}^l(n)$ . Therefore, a sub-optimum scheme which maximizes  $\Lambda_{L_c}^l(n)$  to find the estimated timing offset can be realized with some performance/complexity trade off. The simplified implementation can be achieved by retaining the correlation calculating part and omit the power calculating part in Fig. 4.

### C. Sub-optimum Approach Based on SCCL Algorithm

In order to simplify the above implementation, we adopt a sub-optimum tracking algorithm, SCCL.

#### The Algorithm of SCCL:

- It separates the whole observation interval to many sub-observation intervals.
- In each sub-observation interval, the SCCL inspects three possible linked candidates and choose the one with the maximum likelihood function as the winner.
- In next sub-interval, the winner and two of its linked neighboring candidates are inspected and the one with the maximum likelihood function is chosen as the new winner.
- The process proceeds.

Please note that the likelihood function in SCCL is exactly the log-likelihood function in the above optimum scheme. What we need to do is to change the parameter from  $\tau$  to the timing offset candidate  $\hat{\tau}_l$  which is the estimation of the  $l^{\text{th}}$  sub-observation interval results form the previous symbol.

$$\Lambda_L^l(\hat{\tau}_l + j) = \frac{2}{N} \sum_{k=0}^{N-1} \Re[R_{l,k}^*(\hat{\tau}_l + j)Y_{l,k}(\hat{\tau}_l + j)] - \sum_{n=0}^{N-1} |r(lN + n + \tau)|^2 \quad (9)$$

Where  $\hat{\tau}_l \in \{0, 1, \dots, N-1\}$  is the timing estimation of SCCL at the  $l^{\text{th}}$  sub-observation interval. And  $j \in \{-1, 0, 1\}$ . Also note that  $Y_{l,k}(\hat{\tau}_l + j)$  just denotes the correlation of the advanced version of the received signal corresponding to the  $(\hat{\tau}_l + j)^{\text{th}}$  timing candidate with the  $k^{\text{th}}$  subcarrier at the  $l^{\text{th}}$  symbol period at the receiving end. Assume the sub-observation interval is  $T$ . The block diagram of the proposed SCCL scheme is shown in Fig. 6. Moreover, because the SCCL-based synchronizer only needs to calculate tree likelihood function values in a symbol duration, the implementation in Fig. 6 can be greatly simplified by adopting single branch and reusing the functional blocks of the demodulator.

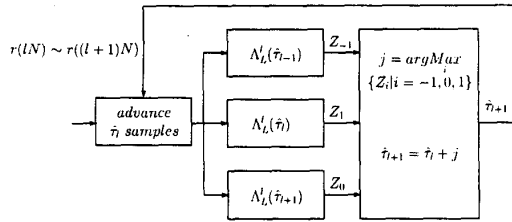


Fig. 6. The block diagram of the proposed SCCL scheme.

#### IV. PERFORMANCE SIMULATION

##### A. The Optimum Synchronizer in open loop operation

An OFDM system consisting of 64 subcarriers and the modulation scheme of QPSK is considered here. White, complex Gaussian noise is added and the normalized mean squared error as a function of the signal to noise ratio is simulated. The signal to noise ratio is defined as

$$SNR = \frac{E\{|s(k)|^2\}}{N * E\{|n(k)|^2\}} = \frac{\sigma_s^2}{N * \sigma_n^2} \quad (10)$$

where  $E\{|s(k)|^2\}$  and  $E\{|n(k)|^2\}$  denote the average symbol power and average noise power respectively. Each value of SNR is simulated for 10,000 symbols. The simulation results are shown in Fig. 7, where we use the sub-optimum scheme which maximizes  $\Lambda_{L_c}^l(n)$  as a reference system.

The tendency of the curves of both the optimum scheme and the sub-optimum scheme basically coincides with the adopted decision directed approach. For  $SNR < 5$  dB, the normalized mean squared error of the estimated timing maintains a level of about  $10^{-1}$  of  $(1/\text{symbol period})^2$ . This tallies with the fact that the feed-backed decision in such SNR condition has a significant error within. While for  $SNR > 7$  dB, the normalized mean squared error of the estimated timing decreases sharp, and for  $SNR > 9$  dB, the simulated normalized mean squared error of the estimated timing equals to zero. This shows that when the error in the feed-backed decision less than a specific level, we can find a dramatically elevation of the performance of the optimum synchronizer. Compared to the optimum scheme, the sub-optimum implementation has little performance difference

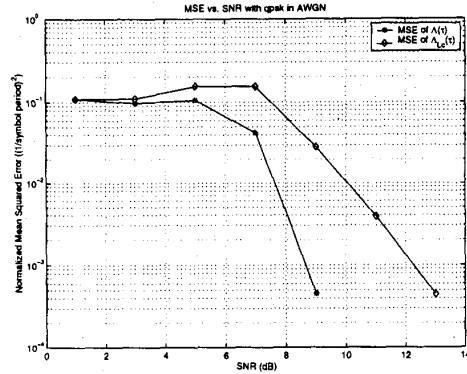


Fig. 7. Normalized mean squared error of the timing estimation vs SNR in AWGN.

for low SNR environment, while for high SNR, it is about 2 dB in average inferior to the optimum synchronizer.

Another simulation about the comparison of normalized mean squared error of the estimated timing versus SNR and the number of subcarriers is illustrated in Fig. 8. The simulation result shows that the proposed synchronizer can get superior performance with a larger number of subcarriers. The performance gap between systems with  $N=64$ ,  $N=128$ , and  $N=256$  is about 1.5 dB/double.

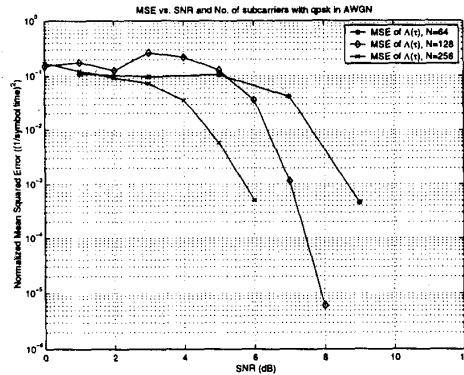


Fig. 8. Normalized mean squared error of the timing estimation vs SNR and No. of subcarriers in AWGN.

##### B. SCCL Synchronizer in closed loop operation

The mean acquisition time of the proposed SCCL-based synchronizer operates in a closed loop environment with initial residual timing offsets of 17, 20 and 31 samples is shown in Fig. 9. Where we assume  $SNR=0$  dB, 2048 subcarriers and QPSK modulation in AWGN channel. Compared to [3], the proposed SCCL-based synchronizer has better performance with 17 samples of residual timing offset and is simpler with the single branch implementation.

## V. CONCLUSION

In this paper, we have proposed a novel symbol timing recovery scheme for OFDM system with a pure digital realization. The proposed optimum scheme is derived based on maximum likelihood criterion with decision feedback and requires no further pilots to assist the estimation. Two sub-optimum schemes, one based on correlation extraction, while the other based on the SCCL algorithm are also developed. Simulation results show that the proposed optimum scheme has excellent performance in estimation variance for SNR > 6 dB in AWGN and the correlation extraction based sub-optimum approach has simplified structure at the price around 2 dB away from optimal value. The SCCL-based sub-optimum approach with simpler implementation is also shown to be effective in closed loop operation.

## APPENDIX

Based on ML criterion, The log-likelihood function corresponds to the  $l^{th}$  symbol can be derived as follows.

$$\begin{aligned}\Lambda^l(\tau) &= \exp\left\{-\frac{1}{N_0} \int_{T_o} |r(t) - s(t - \tau)|^2 dt\right\} \\ &= \exp\left\{-\frac{1}{N_0} \int_{T_o} |r(t)|^2 dt + \frac{2}{N_0} \Re\left[\int_{T_o} r(t)s^*(t - \tau) dt\right]\right\}\end{aligned}\quad (A.1)$$

where  $N_0$  is the one-sided power spectrum density of noise,  $T_o$  is the observation interval and we assume  $T_o \in [lT + \tau, (l + M)T + \tau]$ , with  $M$  a positive integer. And the log likelihood function is

$$\Lambda_L^l(\tau) = 2\Re\left[\int_{T_o} r(t)s^*(t - \tau) dt\right] - \int_{T_o} |r(t)|^2 dt \quad (A.2)$$

we denote the first term in (A.2) by  $\Lambda_{Lc}^l(\tau)$  and it can be further derived.

$$\begin{aligned}\Lambda_{L2}^l(\tau) &= 2\Re\left[\int_{\tau}^{MT+\tau} r(t) \frac{1}{N} \sum_{l=0}^{M-1} \sum_{k=0}^{N-1} X_{l,k}^* e^{-j2\pi f_k(t-\tau)} g(t - \tau - lT) dt\right] \\ &= \frac{2}{N} \sum_{l=0}^{M-1} \sum_{k=0}^{N-1} \Re[X_{l,k}^* \int_{lT}^{(l+1)T} r(t + \tau) e^{-j2\pi f_k t} dt] \\ &= \frac{2}{N} \sum_{l=0}^{M-1} \sum_{k=0}^{N-1} \Re[X_{l,k}^* Y_{l,k}(\tau)]\end{aligned}\quad (A.3)$$

where  $Y_{l,k}(\tau)$  is given by

$$Y_{l,k}(\tau) = \int_{lT}^{(l+1)T} r(t + \tau) e^{-j2\pi f_k t} dt \quad (A.4)$$

Please note, in the above derivations, we neglect all the multiplicative and constant terms since they have no influence on the estimation of the parameter. And if we choose  $M$  to be 1, the log-likelihood function becomes

$$\Lambda_L^l(\tau) = \frac{2}{N} \sum_{k=0}^{N-1} \Re[X_{l,k}^* Y_{l,k}(\tau)] - \int_{lT}^{(l+1)T} |r(t + \tau)|^2 dt \quad (A.5)$$

Based on the decision directed approach, which is to assume  $X_{l,k}$  has been estimated in the absence of demodulation errors, i.e.,  $X_{l,k} = R_{l,k}(\tau)$ , where  $R_{l,k}(\tau)$  is the demodulated symbol from FFT processor corresponding to the timing delay  $\tau$ . Therefore the log-likelihood function becomes

$$\Lambda_L^l(\tau) = \frac{2}{N} \sum_{k=0}^{N-1} \Re[R_{l,k}^*(\tau) Y_{l,k}(\tau)] - \int_{lT}^{(l+1)T} |r(t + \tau)|^2 dt \quad (A.6)$$

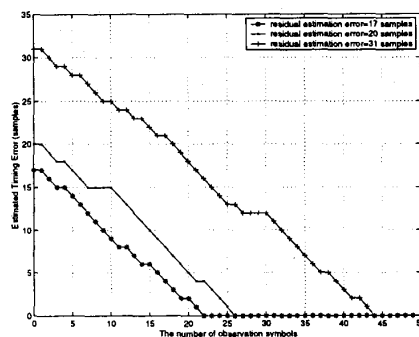


Fig. 9. Mean acquisition time of SCCL with residual estimation error = 17, 20, 31 samples and SNR = 0 dB in AWGN.

## REFERENCES

- [1] A. Pollet and M. Ruiz, "Frequency domain data transmission using reduced computational complexity algorithms," in *Proc. IEEE Int. Conf. Acoust., Speech, Signal Processing*, pp.964-967, Denver, CO, 1980
- [2] B. Marti et al., "European activities on digital television broadcasting from company to cooperative projects," *EBU Technical Review*, no.5, pp.09, 1993.
- [3] D. Lee and K. Cheun, "A new symbol timing recovery algorithm for ofdm systems," *IEEE Trans. Consumer Electronics*, vol. 43, no. 3, pp. 767-775 Aug. 1997
- [4] H. L. Van Trees, *Detection, Estimation, and Modulation Theory (I)*, Wiley, 1968
- [5] J.G. Proakis, *Digital Communication Sed.*, McGraw-Hill, 1995.
- [6] K. C. Chen and L. D. Davisson, "Analysis of a new bit tracking loop - SCCL," *IEEE Trans. Commun.*, vol. 40, no. 1, pp. 199-209, Jan. 1992
- [7] L. J. Cimini, Jr., "Analysis and Simulation of a digital mobile channel using orthogonal frequency division multiplexing," *IEEE Trans. Commun.*, COM-33, no. 7, pp. 665-675, Jul. 1985
- [8] M. Alard, R. Lassalle, "Principles of modulation and channel coding for digital broadcasting for mobile receivers," *EBU Review*, no. 224, pp. 3-15, Aug. 1987.
- [9] P. S. Chow and J. C. Tu and J. M. Cioffi, "Performance evaluation of a multichannel transceiver system for ADSL and VHSLS Services," *IEEE J. Sel. Areas Commun.*, vol. 9, no.6 pp. 909-919, Aug. 1991.
- [10] R. W. Chang, "Synthesis of band-limited orthogonal signals for multichannel data transmission," *Bell System Tech. J.*, vol. 45, pp. 1775-1796, Dec. 1966.
- [11] S. B. Weinstein and P. M. Ebert, "Data transmission by frequency-division multiplexing using the discrete Fourier transform," *IEEE Trans. Commun.*, COM-19(5), pp. 628-634, Oct. 1971.
- [12] T. Pollet and M. Moeneclaey, "Synchronizability of OFDM signals," in *Proc. Globecom'95*, vol.3, pp. 2054-2058, Singapore Nov. 1995